CHEMISTRY OF ASR-GELS AND PORE FLUIDS IN ULTRA-ACCELERATED MORTAR BARS: EVIDENCE FOR SI-CONTROL ON GEL EXPANSION PROPERTIES

Per Hagelia[1,*]
[1]Tunnel and Concrete Division, Technology Department,
Norwegian Public Roads Administration, P.O. Box 8142 Dep, N-0033, OSLO, Norway

Abstract

The chemistry of ASR gels in AAR-2 mortar bars and pore fluids expressed from a parallel series of mortars in 1N NaOH at 80 °C varied systematically with expansion at 14 and 28 days. Pore fluid Si and expansion rates increased linearly with total mortar bar expansion up to about 0.3 % irrespective of age, reflecting aggregation of a viscous Si-O-OH network by Ca-cross linking and supply of free negative surface sites. At expansions > 0.3 % pore fluid Si increased dramatically whilst expansion rates dropped. The swelling potential was controlled by electrical double layer repulsion (alkali/Ca in gels). High swelling pressures can apparently only develop in highly polymerised Si-rich liquid poor gels. Unlike field concrete, ultra-accelerated testing is characterised by a continuous supply of an external extremely alkaline pore fluid at high temperature causing extensive ettringite dissolution. Small differences in expansion between aggregates should not be regarded as significant.

Keywords: Pore fluid & gel chemistry, expansion, silicium, Ca-cross linking, Van Der Waals attraction

1 INTRODUCTION

Alkali Silica Reaction (ASR) occurs in Portland cement based concretes due to kinetic dissolution of silica and formation of variably expansive C-K-N-S-H gels (ASR-gels). The reaction is sustained by the pore fluid composition, which is characterised by pH ≥12.5, leading to high solubility of quartz and amorphous silica. Due to rather slow reaction kinetics only fine grained to cryptocrystalline silica dissolves significantly (cf. Dove and Rimstidt [1]). Aggregate minerals such as feldspars and mica may leach alkalis, which in addition to the cement derived alkalis rises pH in the pore fluid and enhances ASR (cf. Constantiner and Diamond [2]; Bérubé et al. [3]). A prerequisite for expansive behaviour and cracking is that the gels are in a viscoelastic state and a mechanism exists which sustains build up of swelling pressure and internal stress gradients within concrete.

Breakdown of silica takes place in two principal steps [1]; firstly the hydroxyl ions attack the siloxane bridges (Si-O-Si) forming *unstable sites* consisting of a surface layer predominated by silanol groups (Si -OH) at the interface with the liquid. Subsequently *dissolution* takes place due to continued attack of OH^- ions on the unstable sites, with contemporaneous adsorption of molecular water to the silica surface layers. Such water is oriented and hence different from bulk water: In the presence of molecular water the silanol groups become ionised and dissociate. Dissociation leads to deprotonation and formation of motile protons, which upon diffusion creates a pH dependent negative surface charge and a potential. This surface charge strongly attracts monovalent cations and to a lesser extent bivalent ions, forming a diffuse electrical double layer. Formation of $H_4SiO_{4\ (aq)}$ (the monomer $Si(OH)_4$), representing the first dissolution step, is permitted at pH ≈ 9. At yet higher pH a further cascade of dissociation reactions is taking place. This involves deprotonation of H_4SiO_4 and successive formation/deprotonation of $H_3SiO_4^-$, $H_2SiO_4^{2-}$ and $HSiO_4^{3-}$ as pH increases to ≥ 12 [1].

These successive reaction products represent weak acids and result in increasing silica solubility at increasing pH due to buffering by OH, which is typically dependent on the alkali contents in concrete pore fluids. Silica dissolution is further assisted by the presence of cations which may form complexes with the ionised silica species. Ca^{2+} has a much higher affinity for reaction with $H_3SiO_4^-$ and the higher dissociates than Na^+ [1]. Iler [4] found that ionized polymers such as $H_6Si_4O_7^{2-}$ coexist with silica monomers and dimers and increase in abundance at very high pH, notably in presence of amorphous silica. Although some amorphous silica may occur in natural quartz, also the dissolution processes itself involve amorphisation of crystalline silica (Bulteel et al. [5]). Apparently coexistence of monomers, dimers and polymers represents a characteristic feature of early stage ASR irrespective of the type of silica involved.

* Correspondence to: per.hagelia@vegvesen.no

Gels are very low permeable bi-continuous liquid-solid systems of colloidal dimensions: one can move from the solid into the liquid without moving as far as a micron. Gels are very far from equilibrium and highly energetic. The bonding reactions in gels are virtually irreversible; otherwise no such energetic substance could possibly form. Gelation is a process which involves aggregation of polymers forming an increasing fraction of the colloid (sol), which eventually fills space completely as a substance with low fractal dimension forming an elastic gel. The gel elasticity modulus increases in proportion to the volume fraction of the solid (cf. Scherer [6]). Kawamura and Iwahori [7] found that some very alkali rich gels had a very low swelling pressure although the free swelling potential was high, whilst gels with moderate to low alkali contents exerted a pressure. These results seem compatible with investigations by Moore [8] who found that the viscosity of gels increased strongly with increasing SiO_2/H_2O ratios in gels within a rather restricted range of sodium contents coinciding with pH ≈ 12-14. High sodium contents however yielded low viscosities irrespective of gel water contents. Despite this, ASR research has not focused on the significance of SiO_2/H_2O ratios in gels.

Powers and Steinour [9] developed a model which explains the swelling pressure as due to osmosis and water absorption, and also stated that Ca rich gels were non-expansive. However, instead of a semi-permeable layer Dent Glasser and Kataoka [10] invoked differences in chemical potential gradients in the vicinity of reactive silica. Build up swelling pressure was interpreted to be due to water imbibition according to the neutralization principle. Later on Helmut and Stark [11] presented a model based on interpretation of published chemical data, that ASR gels at micro scale represent a two phase system consisting of a non swelling stiff Ca–rich gel and a "mobile" swelling alkali-silica gel: Overall gels with high Ca and low alkali/Si ratios were regarded as very viscous and swelling. This generalisation has however been questioned by Diamond [12], as based on later gel chemical data.

Several authors refer to observations that alkalis seem to penetrate "more deeply" into gels than calcium, emphasising differences in ionic radii and concentration gradients (cf. Wang and Gillott [13]; Chatterji and Thaulow [14]). Chatterji (cf. [14], and references therein) has presented a swelling mechanism where hydrated ions move from low to high concentration regions. This contrasts with the osmotic pressure hypothesis, stating that "expansion occurs when more Na, Ca, OH- and water enters a reactive grain than silica diffuses out" [14].

Ca and portlandite play a significance role in ASR ([14], [12]). An important point is that some Ca is necessary for the formation of gels, otherwise silica would dissolve in the high alkali solution (Thomas [15]). Ca^{2+} ions are derived from dissolution of portlandite in amounts equivalent to the alkali contents in the cement pore fluid thus providing more OH^-. According to [14] portlandite accelerates the penetration of Na, Ca, OH- and water into reactive grains and hampers diffusion of silicate ions from reactive sites.

Recently, Prezzi et al. [16], [17] argued that the gel swelling was caused by electrical double layer repulsion forces similar to clay swelling. Thus mortar bar expansion was found to increase with the ratio of monovalent to bivalent ions in gels. Dissolved silica species have much higher negative surface charge density than the cement hydrates and were regarded as a colloidal suspension. This model is consistent with established silica dissolution mechanisms, and also explains why Na^+ and K^+ are more strongly attracted to the negatively charged hydrated silica surfaces than Ca^{2+}.

1.1 Objectives

The present work focused on the ultra-accelerated mortar bar test method (AAR-2). The main objectives were to: a) investigate time dependent chemical evolution of ASR gels and pore fluids, b) compare this with mortar bar expansion and c) discuss the gel formation and swelling processes and the role of silicium in ASR in the light of proposed models. The results were also used to address the significance of ultra accelerated testing versus real aggregate performance in field concrete.

2 MATERIALS AND METHODS

Three different rock types: 1) Sample 229, Tonalitic mylonite-ultramylonite, 2) Sample 230, Meta-rhyolite conglomerate and 3) Sample 276, Granitic mylonite were selected on the basis of petrographic variation and reactivity. Standard geological nomenclatures (cf. Gjelle and Sigmond [18]) were used for rock classification according to the Norwegian petrographic method [19].

The rock samples were crushed in a jaw crusher and used as aggregates in RILEM AAR-2 *mortar bars* (40x40x160 mm) with w/c = 0.45 and 1.00 % Na_2O_{eq} according to Norwegian procedures (e.g. Lindgård et al. [20]). A *parallel sample series* including reference samples of pure cement pastes was prepared for *pore fluid extraction*. Two specimens of each mix, one for 14 days exposure and the other for 28 day, were moulded in cylindrical 100 ml plastic bottles (inner diameter 47 mm x 58 mm), stripped and exposed to the same accelerated conditions in 1 N NaOH at 80 °C. Exuded hydrous gels

were carefully removed from the cylinders outer surfaces with a scalpel after 14 and 28 days, weighed and stored in tight containers filled with toluol. Mortar bars were washed with distilled water whilst mortar- and paste cylinders were stored in their original NaOH solutions in jars with tight lids. All samples were stored in a dark room at 5 °C for about 3 months before further preparation and analysis, thus lowering the quartz dissolution rate by 4-5 orders of magnitude relative to 80 °C, cf. [1]).

Two series of thin sections were prepared. One series made from the pristine 2-4 mm aggregate size fraction was used for classification of alkali reactivity (cf. Norwegian Concrete Association [19]), quartz grain size measurements and classic petrography, using a polarising microscope with reflected light option. Standard fluorescent epoxy impregnated polished thin sections were made from mortar bar halves cut along their axes (representing 14 and 28 days of exposure), and used for petrography and Back Scatter imaging in conjunction with EMPA. The remaining halves were prepared as plan sections with Epodye for inspections in UV light ("blacklight blue" tubes with peak intensity at 365 nm and a blocking yellow filter at 540 nm). The aggregate mineral composition was analysed semi-quantitatively by X-ray diffraction (XRD) according to procedures at the University of Oslo, using a Philips X'Pert spectrometer.

Pore fluids were extracted from each cylinder at room temperature (20 °C) by a conventional pressure method at 350-400 MPa (cf. Larsen [21] for details). The extraction time was ca 10-15 minutes and the amounts of extracted pore fluids were 2.2 - 4.2 g (mortars) and 6.2 - 6.4 g (pastes). Pore fluids and surface gels were analysed for Ca, Na, K, Si and S by Inductively Couples Plasma II Atom Emission Spectrophotometry in a Perkin Elmer Plasma ICP-AES instrument. Al was analysed by Electro Thermal Atomic Absorption Spectrophotometry in a Perkin Elmer Zeeman 5100 EAAS instrument. Gel data (mg/g) were converted to wt % oxides: Differences from 100 % essentially represent water. Pore fluid OH^- concentrations were obtained by titration using a 716 DMS Titrino instrument. The anion – cation balance was within + 4.9 % to -2.5 % at 20 °C, as calculated by the PHREEQC vs. 2.12.04 computer code (database llnl.dat) assuming pe = -4 and S as sulfate. Saturation indices at 5, 20 and 80 °C indicated that ettringite and quartz were well undersaturated whilst portlandite was saturated.

Electron microprobe analysis (EMPA) of ASR gels and a few precipitates was performed on selected carbon coated thin sections from the mortar bars using a Cameca Camebax instrument. *Selected analysed micro domains*, each of which *covered a full volume of dense gel without visible voids and cracks*, were 5x5 μm^2 squares or 2 μm^2 spot analyses. Smaller gels were skipped. The beam current was 9.2-9.3 nA and accelerating voltage 15 kV. Na was detected second in the analytical sequence and reanalysis of a few micro domains indicated that Na concentrations had not dropped significantly. Each individual analysis was carefully checked by EDS, ensuring that all elements of significant quantity were included. The analysis totals of ASR-gels were always less than 100 %, thus providing additional very important information on the liquid contents of individual gels. The difference from 100 % essentially represents structurally bound- and confined gel water, and likely also non bound water in capillary pores having been replaced by epoxy during preparation.

3 RESULTS

3.1 Aggregate characteristics, mortar bar petrography and UV assessment

The petrographic data from pristine aggregates in Table 1 were based on Hagelia [22]. All samples were rich in quartz and feldspars, yet with differences in mineralogy and grain size. Microscopic assessment in polarising/reflected light and XRD indicated that neither pyrite nor other sulfur bearing phases were present in any of the samples. The pristine grain boundaries were not very accentuated implying generally strong materials. This was confirmed by the jaw crushing. Indeed sample 230 was extremely difficult to crush (O. Muri, Pers. Comm. 1996).

Polarising microscopy, BSE imaging and UV inspection of mortar bar thin- and plan sections focused on the qualitative aspects of ASR reaction products, micro cracking and characteristics of the cement paste matrix. Expansion results are included in Table 2. In UV light the *most expanded (reacted) samples, Series 229 and 230* displayed an outer porous reaction zone increasing in width, from about 2-3 mm at 14 days to 4-5 mm at 28 days. Gels were most abundant within this zone, yet also occurring scattered about within their central domains. *The amount of ASR gel and micro cracking increased relatively with exposure time;* within individual sample series and with total overall expansion. It was also implied but not proven that much of the gel mass occurred at sub microscopic size along mineral grain boundaries, and that the more massive forms represented localised accumulations. Series 229 and 230 were generally characterised by pale to brownish gels in air voids and cracks with darker gels within aggregate particles. Some air void gels in Series 229 and 230 were somewhat porous, notably in 230 after 28 days. In Series 229 some late stage fibrous dense precipitates had formed after ASR gels.

Occasionally in series 229 and 230 an interesting opaque (e.g. in plane polarised light) irregular material occurred within air voids after gel deposition. *In the least reacted Series 276* only a few visible transparent gels were found as air void rims at 14 days, whilst the 28 days sample contained several transparent gels rimming air void; a few thin dark gels occurred within some aggregate particles. In UV light the paste was mostly dark with low porosity.

In Series 229 and 230 the cement paste matrix was brownish light coloured in plane light also within the outer reaction zones. In contrast Series 276 was characterised by an ordinary dark paste, being quite similar to unaffected concrete. Primary well disseminated fine grained *portlandite* occurred in Series 276 but was apparently much less abundant in Series 229 and 230 and possibly decreased from 14 to 28 days. Fibrous crystalline reaction products, some of which resembled ettringite, postdated gels within air voids in the most reacted samples.

In contrast to the pristine samples, cracking of aggregate particles within in the mortar bars was developed along quartz- and other grain boundaries. This was sometimes characterised by a connecting network of open channels, most typically developed within series 229 and 230 after 28 days of immersion. Although crack bound gels also occurred the majority of channels were empty.

3.2 Chemical variation of pore fluids and reaction products compared to total expansion

The chemistries of pore fluids, gels and precipitates are given in Tables 2, 3 and 4. The pore fluids represent average compositions from a large volume of each cylindrical specimen and were therefore compared to the arithmetic mean composition of individual *internal* gels (e.g. in air voids, within aggregate particles and cracks in paste) in each mortar bar sample: It is admitted though that the statistical basis is a bit poor and that variation of individual gel compositions in each sample overlapped to a great extent. *Exuded gels* and internal *precipitates* were assessed separately.

Silicium and the liquid component

Figure 1A shows that the total dissolved Si in pore fluids from all samples increased linearly with total expansion up to about 0.3 %, irrespective of age. The expansion rate also increased linearly. At expansions > 0.3 %, represented by samples 229 and 230 after 28 days of exposure, the dissolved Si increased about an order of magnitude while their expansion rates dropped from about 0.02 (%/day) at 14 days to 0.009 at 28 days. The averaged SiO_2 contents in internal gels apparently increased asymptotically towards a maximum concentration of about 60 wt % SiO_2 up to about 0.3 % total expansion (Figure 1B). Only sample 230 showed a clear drop in the SiO_2 contents at 28 days (> 0.35 % total expansion). In contrast the SiO_2 contents in exuded surface gels were very low, reaching about 5 wt % in the most reacted samples. These gels were very hydrous (82-87 wt %), whilst exuded deposits on samples 276 were much less hydrous and rich in Ca (Table 4). The late stage precipitates in 229 apparently represented a form of impure silica with SiO_2 contents ranging from 64 to 89 wt % and "water" ranging from 5.6 to 15.8 wt %. Opaque reaction products represented pure silica.

There was a very good negative linear correlation (R^2 = 0.92) between SiO_2 and "Water" (Figure 1C). A nearly identical correlation (R^2 = 0.73) was found for all individual gel analyses (not shown). In a rough sense the liquid component decreased with rising total expansion and expansion rate up to ≈ 0.35 %, except for sample 230 at 28 days with high "water" contents (Figure 1D).

Alkalis, OH^-, calcium and pH

The total alkali concentrations ([Na]+[K]) and [OH^-] in pore fluids displayed a coherent pattern, showing a steep positive linear relationships against total expansion (Figures 1 E and 2A). Sample 230B consistently fell off the trends at higher concentrations. There is however an important difference between the two parameters: at zero expansion the alkali trend intersected at alkalis ≈ 1 mol/L similar to the NaOH bath, whilst [OH^-] intersected at 0.8 mol/L. The alkalis increased progressively with total expansion to concentrations exceeding that in the surrounding NaOH bath, whilst the [OH^-] increase never reached 1 mol/L, except for in 230B. The alkali and OH^- contents in the reference pastes increased with time (14 to 28 days) from about 1.1 to 1.2 mol/L and 0.8 to 1 mol/L, respectively, hence spanning most of the variation.

The total alkali contents in the internal gels (Figure 1F) ranged from 2-8 wt % and increased linearly with total expansion. Yet sample 230B at highest total expansion deviated from the general trend at a relatively lower alkali content. Na/K ratios usually increased somewhat from 14 to 28 days. The late stage internal precipitates in Series 229B contained more sodium than potassium in contrast to the gels. The exuded surface gels contained about 2-7 wt % Na_2O whilst K_2O was very low.

Ca in pore fluids (Figure 1G) showed an overall depletion trend versus expansion, with the highest concentrations in the reference pastes and the lowest concentrations in the most reacted

mortars. In the least reacted sample series 276, Ca increased from day 14 to day 28 reflecting similar behaviour as reference pastes, whilst in sample series 229 and 230 the Ca was decreasing. The internal gels also showed a steady drop in CaO wt % up to a total expansion about 0.3 %, whilst the two most reacted samples showed a constant Ca (230B) or relative increase (229 B) at the highest total expansion level (Figure 1H). The exuded gels from samples 229 and 230 had low CaO contents and yet Ca/Si ratios ≈ 1: about 3-4 times higher than the internal gels. The precipitates had rather low CaO yet similar to some internal gels in sample 229. pH generally increased slightly with age.

Sulfur and aluminium

The S contents in pore fluids were very high also in the reference pastes. Sulfur contents increased roughly with total expansion. As regards compositions of gels and precipitates sulfur contents were low. The pore fluids were low in Al but the contents generally increased with expansion. Similarly Al_2O_3 (wt %) in gels was quite low. The lowest Al contents were in precipitates and exuded gels (cf. Tables 2, 3 and 4). One ettringite like deposit in sample 230 was analysed by EMPA showing it was an ASR reaction product. It is possible that many of the secondary air void deposits resembling ettringite in fact were crystallised gels.

3.3 Calculation of charge fractions of bivalent cations in gels

The charge fractions of bivalent cations (E_{BIV}) Ca^{2+}, Mg^{2+} and Mn^{2+} (assuming reducing conditions) were calculated for gels and precipitates according to the following equation (cf. [17]) (Tables 3 and 4):

$$E_{BIV} = \frac{molCaO + molMgO + molMnO}{molCaO + molMgO + molMnO + molNa_2O + molK_2O} \quad (1)$$

where "mol" refers to the number of moles of an oxide component. Internal gels show a negative correlation between E_{BIV} and expansion: at 14 days expansion samples plot on a less steep trend than the 28 days results, being parallel to the 30 days results of Prezzi et al. [17] (Figure 2B).

4 DISCUSSION

4.1 Introduction

The present results reflect essential chemical phenomena of ASR described by previous workers as referred to above. Expansion was negatively correlated with quartz grain size and the amount of ASR gel formed had increased with total accumulated expansion (see also Kawamura and Iwahori [7], Hagelia [23]. However this work has unveiled systematic changes in pore fluid concentrations and complimentary changes in the ASR-gel compositions which have not been reported earlier. Apparently these features reflect fundamental processes in the gel-fluid system. A new model for ASR gel aggregation, development of viscoelasticity and swelling capacity has been established below, which is at least relevant for the ultra-accelerated test method.

The very high pore fluid pH (Table 2), about one unit higher than in field concrete, suggests that the quartz dissolution rate was maintained at a the same level throughout the experiment. The linear correlation between dissolved silica species and expansion up to about 0.3 % suggests that the first stage was characterised by a "steady state" where dissolved Si was incorporated into ASR gel at a quite constant rate (Figures 1A, 1B), taking into account that gel volume roughly increased with total expansion. The subsequent dramatic increase in pore fluid [Si] at > 0.3 % expansion is quite obviously evidence for depletion or exhaustion of a Ca source: A similar effect resulting in even more extreme [Si] has been reported from an aggregate immersion experiments in 1N NaOH at 80°C without portlandite (Feng et al. [24]).

Ca^{2+} in the pore fluids *originated from both portlandite and primary ettringite:* Breakdown of the siloxane bridges and formation of silanol bonds led to an OH^- deficit relative to Na^+ and K^+, which is apparent from Figures 1E & 2A. Thus quartz dissolution triggered dissociation of *portlandite* and liberation of Ca^{2+} and OH^- to the pore fluid, as corroborated by the depletion of portlandite observed in thin section; simultaneous increase in pore fluid Ca^{2+} and OH^- in series 276 and pastes (Figures 1G, 2A) and previous work on ASTM 1260 mortar bars (Hou et al. [25]). *Extensive dissolution of primary ettringite* took place as suggested by a) the very high S contents in all pore fluids including reference pastes, b) the lack of sulfur bearing minerals in the aggregates and c) significant undersaturation of ettringite as established by PHREEQC modelling (premature though, since reliable thermodynamic data for ASR gel is lacking). The extremely high S contents in 229B and 230B pore fluids implies that Ca at this stage was perhaps mostly derived from ettringite, in keeping with recent experiments by

Shimada and Young [26]) using 1 NaOH at 80 °C. The low Al contents in pore fluids and most gels suggest that Al liberated from ettringite was trapped in a cement hydrate, possibly the U-phase [26].

The coherent increase of Na^+ and OH^- in pore fluids and notably the abrupt rise represented by sample 230B needs to be explained (Figures 1E and 2A) since especially Na^+ reached concentrations exceeding 1 mole/L. It seems likely that the contribution of alkalis from cement paste and possibly aggregates increased due to the enhanced mortar porosity associated with increasing expansion. However pore fluid Na^+ might also have been enhanced by its attraction to unsatisfied negative sites on the silica ions, as driven by chemical potential gradients. This effect should be most significant at highest concentrations of dissolved Si which was indeed the case for sample 230B. Thus OH^- in the pore fluid, derived from portlandite and the external NaOH bath, should also rise coherently in an attempt to maintain charge balance. Yet the OH^- deficit was retained, apparently due to simultaneous formation of silanol bonds.

4.2 ASR-gel formation and swelling: a new model

A two component mixture of Si-O-OH and liquid with alkalis attached to electrical double layers

A fundamental aspect of this model is represented by the good inverse linear relationship of gel SiO_2 and "water" in gels, which strongly suggests that *ASR gels consist of two main components; a solid Si-O-OH network and a liquid*. This is very different from the model by Helmut and Stark [11] but compatible with the general gel model of Scherer [6]. There was neither any explicit evidence for water imbibition associated with increasing expansion rates (i.e. up to 0.3 % total expansion). On the contrary, the SiO_2 contents in gels apparently increased asymptotically versus expansion while expansion rates and gel volume increased. As such ASR gels became progressively "saturated" in silicium during build up of viscoelasticity. This feature most likely reflects the condensation reaction (i.e. growth of gel) as it proceeded towards full polymerisation. Evidently quartz dissolution represents the rate limiting step for ASR-gel formation.

A second fundamental feature was that mortar bar expansion increased with a decreasing charge fraction of bivalent cations (E_{BIV}). This is strong evidence in favour of a gel swelling mechanism involving *electrical double layer repulsive forces* (Figure 2B). However the 14 days results fell on a less steep slope than the 28 days results, both at lower E_{BIV} than the 30 days results presented by Prezzi et al. [17]. These differences indicate that ASR gel swelling was not solely dependent on E_{BIV}. It is suggested that quartz dissolution rate, gel aggregation rate, gel volume and gel viscosity also played important roles. The positive linear correlation of alkalis in gels with total expansion (Figure 1F), accompanied by decreasing CaO contents while SiO_2 accumulated in gels (Figures 1B and 1H), suggests that aggregation of the Si-O-OH network steadily supplied unsatisfied negative surface charge with an increasing potential for swelling. It should further be noted that electrical double layers are very thin at high ionic strength and high temperature (cf.[1]). Thus at least in the case of AAR-2, electrical double layers should not readily overlap but exert an important swelling component due to the extremely high Na/Ca ratios involved.

Aggregation and development of viscoelasticity by Ca-cross-linking and Van Der Waals attraction

Viscoelastic gel must have formed by aggregation of a solid Si-O-OH network within an ion rich electrolyte or sol [6, 17]. At an early stage the sol was characterised by elevated contents of Na^+ (K^+), negatively charged Si-complexes (monomers, dimers and polymers), Ca^{2+} and likely sulfate (Table 2). According to Prezzi et al. ([16]) aggregation was due to the effects of Van Der Waals forces becoming effective when silica ions approach each other, likely during the course of a drying event. However in the present authors' opinion the effect of a continuous dissolution of quartz and increasing concentration of silica ions is in itself a way to bring particles to within a distance where Van Der Waals attraction becomes important. ASR gels also usually contain an amount of calcium, which is most frequently higher than the alkali contents as in the present case (Table 3). Since Ca^{2+} is less strongly attracted than Na^+ and K^+ in the double layers this suggests that an appreciable portion of the total calcium was bound to the Si-O-OH network and played a role in gelation. Indeed the electrostatic energy between Ca^{2+} and O^-, i.e. the affinity for reaction with hydrated silica polymers, is greater than Na^+ and K^+ (cf. [13],[1]). Hence, prior to gelation the Ca should be more strongly attracted to the hydrated negative silica ions in solution than the alkali ions, e.g. opposite to the behaviour in electrical double layers. This mechanism seems directly supported by the experiments of Gaboriaud et al. [27] who demonstrated that in a strongly basic silico-alkaline solution the presence of Ca^{2+} ions was promoting cross-linking of silicate ions in the gelation process.

Thus the present author would argue that Ca cross-linking was the most important aggregation mechanism at an early stage, whilst Van Der Waals attraction became increasingly important at later stages characterised by higher dissolved silica concentrations after partial build up of the Si-network. This is corroborated by the overall decreasing Ca contents in gels and pore fluids up to about 0.3 % total expansion (Figures 1G and 1H). The reason for this drop was probably that Ca escaped from the gel-pore fluid system due to pozzolanic reaction forming CSH, and likely also through exudation; the exuded gels had Ca/Si ratios 3-4 times higher than the internal gels (Tables 3 and 4). Yet Ca^{2+} was still available in the pore systems which assisted by Van Der Waals forces steadily build up a Si-network with increasing viscosity. Recent work suggests that well developed Ca free ASR gels consist of SiO^- and Si-OH in roughly equal proportions, with one non-bridging O^- (i.e. unsatisfied negative charge) per Si site in a network involving sheet like and cross polymerisations (Hou et al.[28]]). Since polymers such as $H_6Si_4O_7^{2-}$ become very abundant at highest pH (cf. [4]) it is expected that a rather small amount of Ca is required for their aggregation. Therefore also aggregation of Ca bearing ASR gels should provide unsatisfied negative sites still as the degree of polymerisation increases. Aggregation should eventually lead to complete confinement of liquid at very small scale, such that the gel water becomes isolated from the bulk pore fluid. Na^+ and Ca^{2+} in electrical double layers should cause a high swelling potential. But only in combination with a highly polymerised viscoelastic Si-O-OH network with an appreciable amount of confined liquids the development of high swelling pressures seems possible. The principal aspects of this model are probably also valid for field concrete.

Expansion rate controlled by alkali/Ca ratios and extent of network aggregation

The expansion rates had dropped significantly in samples 229 and 230 at 28 days. Within the framework of the present model a sequential lowering of expansion rate may be the result of: a) lowering of alkali/Ca ratio in the electrical double layers, b) effects of accumulated additional new and less stiff gels with lower degree of polymerisation c) water imbibition and d) partial dissolution of gels. Assuming that the gels have very low permeability and gelation is an irreversible process [cf. 6] the latter two processes seem unlikely. In sample 229B the alkali-oxide/CaO ratio in gels at 28 days was much lower than at 14 days (0.39 and 0.48, respectively) and CaO had increased (Figure 1H) which should lead to a weaker double layer repulsion. As regards sample 230B the explanation is different since the alkali-oxide/CaO ratio here had increased from 0.36 (14 days) to 0.42 (28 days) whilst CaO in gels remained the same. The main difference was much higher gel water content (Figure 1D) suggesting that the lower expansion rate was caused by influence from later formed gel masses with a lesser degree of polymerisation. Yet water imbibition cannot formally be excluded, the effect of which would in case be the reverse of what has previously been suggested.

4.3 Exuded surface gels and internal Si rich precipitates

The exuded very hydrous gels from mortar surfaces apparently aggregated in direct contact with 1N NaOH as indicated by their elevated Na contents. It is considered that they mainly originated from the outer porous zones of the mortars, implying that they had low viscosities and were essentially non-elastic with transitional properties towards the sols they were formed from. The formation of internal Si-rich deposits after ASR-gels were stabilised by an evolved pore fluid chemistry rich in Si and alkalis. In a sense they represent some sort of a complimentary composition to the exuded gels.

4.4 Gel swelling pressures versus tensile strength of concrete and aggregates

Reported ASR-gel swelling pressures at 2-7 MPa (cf. [7][16][23][29][30]) are by some workers regarded as unrealistically low in view of the > 10MPa tensile strength of high quality aggregates. However ASR is a strain softening reaction: breaking of the siloxane bridges and formation of silanol bonds represents a significant chemical softening referred to as hydrolytic weakening (e.g. Griggs [31]). This acts in addition to the effects of *grain boundary dissolution* and *cracking* due to gel swelling. The significant ASR related micro cracking of the initially strong aggregate in sample 230 seems to be a manifestation of these processes. Thus many initially strong ASR susceptible aggregates will eventually crack at gel swelling pressures less than 10 MPa due to hydrolytic weakening and quartz dissolution.

4.5 Comments on the ultra-accelerated mortar bar test: what does it tell?

The ultra-accelerated test method is characterised by abnormally high Na/Ca molar ratios and artificially high ionic strength in pore fluids imposed by an externally very aggressive NaOH solution of fixed composition. Contrary to this available alkalis for ASR in field concretes is at least an order of magnitude lower (cf. data in [3]) and the thermal conditions do not lead to "extra polymerisation"

through release of Ca from bulk scale ettringite dissolution, which is the case in AAR-2. In fact the ultra-accelerated test does neither invoke the effects of real pore fluids nor a real temperature regime. Thus without *a priori* knowledge of the pore fluid composition in a real mix it would seem meaningless to attribute differences of say 0.08 % to 0.10 % expansion as being of any significance.

5 CONCLUSIONS

The chemistry of internal ASR gels in AAR-2 mortar bars and pore fluids expressed from a parallel series of mortars in 1N NaOH at 80 ^{o}C varied systematically with expansion at 14 and 28 days. The Si/"water" ratio in gels apparently had a profound control on expansion and swelling. A new model for gel swelling is proposed which is probably also valid for field concrete: ASR-gels represent a two component mixture of a solid Si-O-OH network and a liquid (gel "water") with alkalies and some of the calcium attached to electrical double layers. The swelling potential was sustained by electrical double layer repulsion governed by alkali/Ca ratios whilst high swelling pressures can apparently only develop in highly polymerised viscoelastic Si-rich and liquid poor gels. Aggregation of the Si-O-OH network was initiated and further sustained by cross-linking of Ca^{2+} ions, followed by an increasing effect of Van Der Waals attraction as the concentration of dissolved silica ions and gel polymerisation increased. ASR is a chemical strain softening reaction leading to weakening of initially strong aggregate particles. Unlike field concrete, ultra-accelerated testing is characterised by a continuous supply of an external extremely alkaline pore fluid at high temperature causing extensive ettringite dissolution. Small differences in % expansion between aggregates should not be regarded as significant.

6 ACKNOWLEDGEMENTS

Most of this work was undertaken at the previous Norwegian Road Research Laboratory (NRRL) during 1996-1998. I wish to thank Erik Endre, formerly with NRRL, for numerous discussions on ASR during the initial years 1993-1996. I am also indebted to: Berit Løchen-Berg and Muriel Erambert (University of Oslo) for XRD analysis and assistance during my EMPA analysis, respectively; Jan Viggo Holm and Oddvar Muri (NOTEBY AS) for accelerated testing and Hilde Johansen (Norsk Analyse Center SERO) for the ICP-AES and EAAS analyses. At NRRL Per Geir Sigursen made the plan and thin sections, Claus K Larsen extracted the pore waters and Bernt Helland analysed for OH^-. Sidney Diamond (Purdue University) is thanked for very fruitful comments. Finally I wish to thank good fortune and the Norwegian Public Roads Adminsitration, Project number P-496 for funding.

7 REFERENCES

[1] Dove, PM and Rimstidt, JD (1994): Silica – water interactions. In: Heaney P.J., Prewitt, C.T. and Gibbs, G.V. (eds.), Silica. Reviews in Mineralogy, (29): 259-308.

[2] Constantiner, D and Diamond, S (2003): Alkali release from feldspars into pore solutions. Cement and Concrete Research, 33, 549-554.

[3] Bérubé, M-A and Fournier, B (2004): Alkalis releasable by aggregates in concrete – Significance and test methods. In: Tang, M. & Deng, M. (editors): Proceedings of the 12th International Conference on Alkali-Aggregate Reaction in Concrete, Beijing, China, Vol. I, 17-30.

[4] Iler, R (1979): The Chemistry of Silica, 2nd edition. John Wiley and Sons, New York: pp 865.

[5] Bulteel, D, Riche, J, Garcia-Diaz, E, Rafai, N and Degrugilliers, P (2004): Better understanding of ASR mechanisms thanks to petrography study on altered flint aggregate. In: Tang, M. & Deng, M. (editors): Proceedings of the 12th International Conference on Alkali-Aggregate Reactions in Concrete, Beijing, China, Vol. I, 69-78.

[6] Scherer, G (1999): Structure and properties of gels. Cement and Concrete Research, 29, 1149-1157.

[7] Kawamura, M, and Iwahori, K (2004): ASR gel composition and expansive pressure of mortars under restraint. Cement and Concrete Composites 26, 47-56.

[8] Moore, AE (1978): An attempt to predict the maximum forces that could be generated by alkali-silica reactions. In: Diamond, S. (ed.), Proceedings of the 4th International Conference on the effects of alkalis in cement and concrete. Purdue University, USA, 363-368.

[9] Powers, TC, and Steinour, HH (1955): An interpretation of some published researches on alkali-aggregate reaction 2 – An hypothesis concerning safe and unsafe reactions with reactive silica in concrete. Journal, American Concrete Institute Proceedings, 51, 785-811.

[10] Dent Glasser, LS, and Kataoka, N (1981): The chemistry of alkali-aggregate reactions. Proceedings of the 5th International Conference on Alkali-Aggregate Reactions in Concrete, Cape Town, South Africa, S252/23.

[11] Helmuth, RA, and Stark, D (1992): Alkali silica reactivity mechanisms. In: Skalny, J. (ed.), Materials Science of Concrete III, American Ceramic Society, 131-208.
[12] Diamond, S (2000): Chemistry and other characteristics of ASR gels. In: Bérubé, M.A., Fournier, B. and Durand, B (editors) Proceedings of the 11th International Conference on Alkali Aggregate Reactions in Concrete, Québec, Canada, 31-40.
[13] Wang, H, and Gillott, JE (1991): Mechanism of alkali-silica reaction and the significance of calcium hydroxide. Cement and Concrete Research, 21, 647-654.
[14] Chatterji, S, and Thaulow, N (2000): Some fundamental aspects of alkali-silica reaction. In: Bérubé, MA, Fournier, B, and Durand, B (eds.), Proceedings of the 11th International Conference on Alkali Aggregate Reactions in Concrete, Québec, Canada, 21-29.
[15] Thomas, MDA (1998): The role of calcium in alkali silica reaction. Materials Science of Concrete: Special Volume – The Sidney Diamond Symposium. Cohen, MD, Mindess, S, and Skalny, JP (eds.), American Ceramic Society, 325-337.
[16] Prezzi, M, Monteiro, PJM, and Sposito, G (1997): Alkali-Silica Reaction – Part 1: Use of the Double-Layer Theory to Explain the Behaviour of Reaction-Product Gels. ACI Materials Journal. Title no. 94-M2, 10-17.
[17] Prezzi, M, Monteiro, PJM and Sposito, G (1998): Alkali-Silica Reaction – Part 2: The Effect of Chemical Admixtures. ACI Materials Journal. Title no. 95-M1, 3-10.
[18] Gjelle, S, and Sigmond, EMO (1995): Classification of rock types and map production. Skrifter 11, Geological Survey of Norway, pp 77 (in Norwegian).
[19] Norwegian Concrete Association (2004): Durable concrete containing alkali reactive aggregates. NB Publication No. 21, pp 22 with appendices (in Norwegian).
[20] Lindgård, J, Dahl, PA and Jensen, V (1993): Rock composition – reactive aggregates: Test methods and requirements to laboratories. SINTEF Report, STF70 A93030, pp 9 (in Norwegian).
[21] Larsen, C (1998): Chloride binding in concrete. Effects of surrounding environment and concrete composition. Dr. Thesis, Norwegian University of Science and Technology, pp 325.
[22] Hagelia, P (1999): Comparison of three test methods for alkali reactivity. Technology Department, Norwegian Public Roads Administration, Internal Report No. 2076, pp 21 + enclosures (in Norwegian).
[23] Hagelia, P (2004): Origin of map cracking in view of the distribution of air-voids, strength and ASR-gel. In: Tang, M. & Deng, M. (eds.) Proceedings of the 12th International Conference on Alkali-Aggregate Reaction in Concrete, Beijing, China, Vol. II, 870-881.
[24] Feng, X, Thomas, MDA, Bremner, TW, Balcom, BJ and Foliard, KJ (2006): Effect of $LiNO_3$ on ASR-induced expansion and dissolution of silica. In: Fournier, B (ed.) Marc-André Bérubé Symposium on Alkali-Aggregate Reactivity in Concrete, Montréal, Canada, 139-152.
[25] Hou, X, Struble, LJ and Kirkpatrick RJ (2004): Formation of ASR gel and the roles of CSH and portlandite. Cement and Concrete Research, 34, 1683-1696.
[26] Shimada, Y, and Young, FJ (2004): Thermal stability of ettringite in alkaline solutions at 80 °C. Cement and Concrete Research, 34, 2261-2268.
[27] Gaboriaud, F, Nonat, A, Chaumont, D and Craievich, A (1999): Aggregation and gel formation in basic silico-calco-alkaline solutions studied: A SAXS, SANS and ELS study. Journal of Physics and Chemistry, 103, 5775-5781.
[28] Hou, X, Struble, LJ and Kirkpatrick RJ (2004): Känemite as a model for ASR gel. In: Tang, M. & Deng, M. (eds.) Proceedings of the 12th International Conference on Alkali-Aggregate in Concrete, Beijing, China, Vol. I, 115-124.
[29] Diamond, S (1989): ASR – Another look at mechanisms. Proceedings of the 8th International Conference on Alkali-Aggregate Reaction in Concrete, Kyoto, Japan, 83-94.
[30] Binal, A (2004): A new experimental method and device for measuring alkali silica gel pressure in mortars. In: Tang, M. & Deng, M. (eds.) Proceedings of the 12th International Conference on Alkali-Aggregate Reaction in Concrete, Beijing, China, Vol. I, 870-881.
[31] Griggs, D.T. (1967): Hydrolytic weakening of quartz and other silicates. Geophysical Journal of Royal Astronomy Society, 14, 19-31.

TABLE 1: Summary of aggregate petrography and % reactive component according to the Norwegian petrographic method. Formation temperatures of mineral assemblages: Sample 276 ≈700 °C; samples 229 & 230 ≈ 500-600 °C (Hagelia [22]). Mu=muscovite, Bi=biotite Qz=quartz, Pl=plagioclase, Or=orthoclase, Mi=microcline, Chl=chlorite, Mt=magnetite, Cc=calcite, Dol=dolomite, Ep= epidote, Ap=apatite, Zr=zircon.

Sample No.	**Rock type**	**Susceptible aggregate**	**Mineralogy**	**Quartz size (D_{50})**
229	Tonalitic (ultra-)mylonite	100 %	Mu+Qz+Pl > Mi+Chl+Mt+Cc+Dol	15 µm
230	Meta-rhyolitic conglomerate	94 %	Mu+Qz+Mi+Pl > Bi >> Cc+Chl+Mt+Ep	13 µm
276	Granitic mylonite	100 %	Pl+Qz+Or >Bi >> (Chl)+Mu+Mt+Cc+Ap+Zr	43 µm

TABLE 2: Chemistry of pore fluids expressed from cylindrical mortars and reference paste exposed to 1 N NaOH at 80 °C (ICP-AES, and EAAS*). pH as calculated from [OH-] is regarded as about 0.2 units higher than real.

Sample	**Exposure time**	**Expansion accumulated**	**Expansion rate**	**Pore fluid chemistry (mg/L)**							
	Days	*%*	*%/day*	*Ca*	*Na*	*K*	*S*	*Si*	*Al**	*OH-*	*pH*
229A	14	0.23	0.017	15.2	23800	900	1200	117	8.3	14951	13.95
229B	28	0.36	0.009	10.2	27300	1090	3600	1108	9.8	15964	13.97
230A	14	0.27	0.019	25.3	25700	1130	2100	148	8.6	14936	13.94
230B	28	0.39	0.009	19.3	34200	1180	4700	1590	16.0	19303	14.06
276A	14	0.08	0.005	41.6	22500	920	1400	33	5.0	13739	13.91
276B	28	0.15	0.005	55.0	24900	690	1600	78	10.3	14904	13.94
Ref A	14	-	-	53.4	24300	1130	2050	7	2.2	13644	13.90
Ref B	28	-	-	84.7	27700	765	1650	14	5.3	17233	14.01

TABLE 3: Chemistry of internal gels in mortar bars (arithmetic mean of several analyses by EMPA). Charge fraction of bivalent cations (E_{BIV}) calculated according to Equation 1. The analytical difference from 100 % essentially corresponds to gel water.

	Gels in 229		**Gels in 230**		**Gels in 276**	
	(n = 5)	**(n = 9)**	**(n = 10)**	**(n = 5)**	**(n= 3)**	**(n = 5)**
Wt.%	14 days	28 days	14 days	28 days	14 days	28 days
Na_2O	1.13	2.92	2.21	3.00	1.64	2.40
K_2O	3.82	4.74	3.38	3.63	0.54	1.95
SiO_2	59.03	56.55	58.01	43.12	42.17	55.06
TiO_2	0.12	0.02	0.02	0.13	0.02	0.03
Al_2O_3	7.43	0.09	0.53	3.00	1.06	0.44
FeO-total	2.27	0.07	0.17	1.52	0.22	0.36
MnO	0.03	0.04	0.02	0.00	0.02	0.01
MgO	0.45	0.01	0.04	0.76	0.23	0.17
CaO	10.23	19.61	15.53	15.75	25.05	20.55
Cl	0.05	0.04	0.05	0.10	0.03	0.09
SO_3	0.11	0.14	0.32	0.34	0.27	0.12
P_2O_5	0.20	0.33	0.26	0.27	0.42	0.33
SUM	84.89	84.54	80.55	71.61	71.67	81.51
100-SUM	15.11	15.46	19.45	28.39	28.33	18.49
E_{BIV}	0.711997	0.765557	0.754398	0.741013	0.934903	0.846573

TABLE 4: Chemistry of exuded gels from outer surfaces of mortars (recalculated from mg/g by ICP-AES and EAAS*) and internal precipitates (EMPA) post dating internal gels. SiO_2 in precipitates ranged from 64 to 89 Wt. %.

	Exuded gels on 229		**Exuded gels on 230**		**Exuded gels on 276**		**Precipitates in 229**
	(0.35 g)	**(0.49 g)**	**(0.49 g)**	**(0.62 g)**	**(0.01 g)**	**(0.01 g)**	**(n = 4)**
Wt.%	14 days	28 days	14 days	28 days	14 days	28 days	28 days
Na_2O	7.18	5.53	5.88	6.12	2.05	2.75	2.33
K_2O	0.07	0.05	0.06	0.06	0.00	0.00	0.77
SiO_2	5.04	4.64	4.06	3.42	0.66	1.26	74.37
TiO_2	0.00	0.00	0.00	0.00	0.00	0.00	0.02
Al_2O_3	* 0.12	* 0.20	* 0.12	* 0.14	* 0.10	* 0.10	0.17
FeO-total	0.00	0.00	0.00	0.00	0.00	0.00	0.10
MnO	0.00	0.00	0.00	0.00	0.00	0.00	0.05
MgO	0.00	0.00	0.00	0.00	0.00	0.00	0.07
CaO	5.36	4.10	5.12	2.84	67.16	60.73	10.42
Cl	0.00	0.00	0.00	0.00	0.00	0.00	0.04
SO_3	0.18	0.11	0.19	0.14	0.00	0.00	0.09
P_2O_5	0.00	0.00	0.00	0.00	0.00	0.00	0.17
SUM	17.95	14.63	15.43	12.72	69.97	64.84	88.60
100–SUM	82.05	85.37	84.57	87.28	30.03	35.16	11.40
E_{BIV}	0.450496	0.448912	0.488745	0.337574	0.973125	0.960642	0.783693

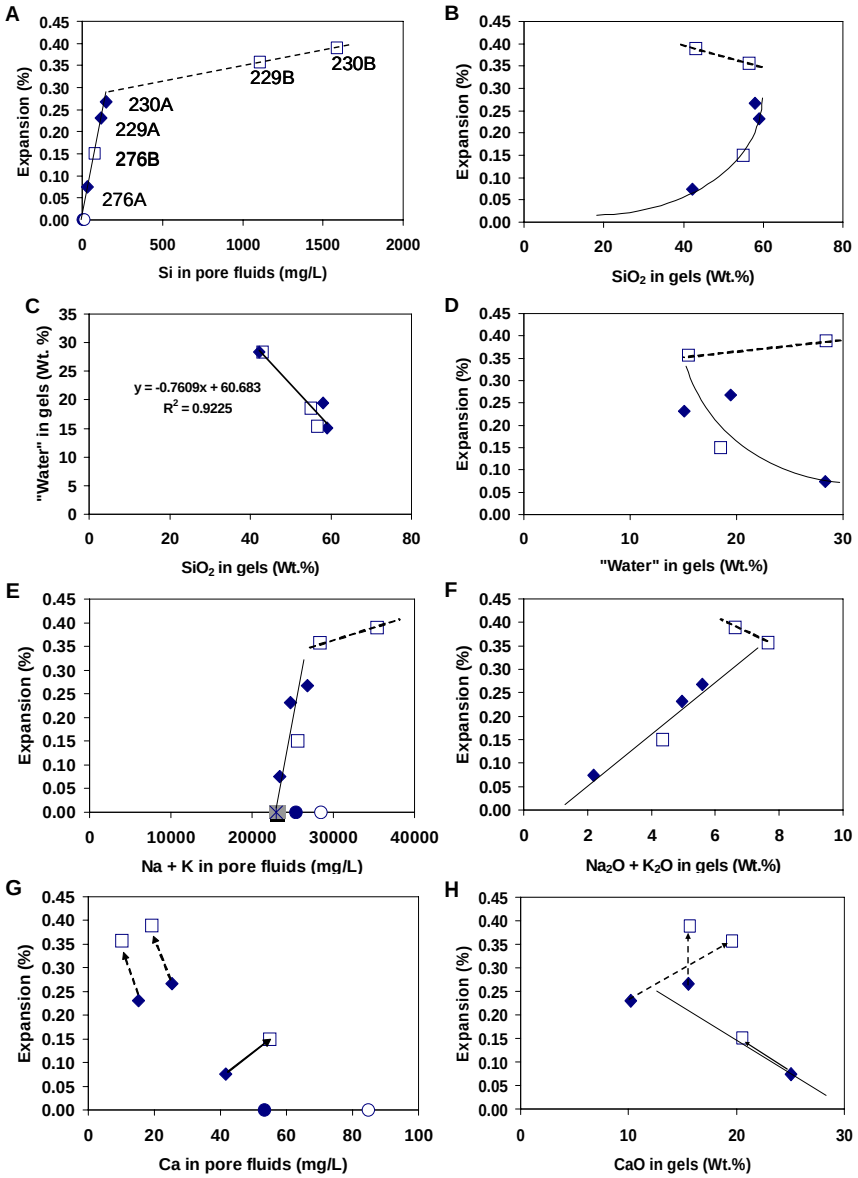

Figure 1: Chemistry of expressed pore fluids (ICP-AES) and averages of internal gels (EMPA) versus total mortar bar expansion at different ages. Symbols: Filled diamonds = 14 days; Open squares = 28 days. Circular = reference cements (filled = 14 days; open = 28 days). Grey square with cross = 1N NaOH. Arrows: evolutionary trends of three sample series 14 → 28 days. Sample numbers as in Table 2.

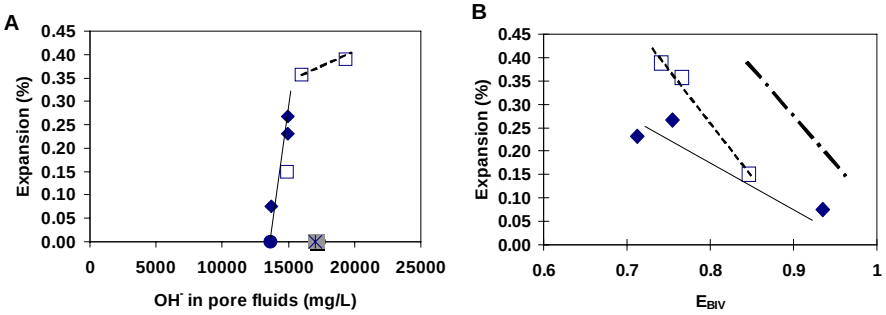

Figure 2A: OH^- in pore fluids. Notice that the concentrations were mostly lower than in 1 N NaOH (28 days reference cement plots at 1N). Figure 2B: Molar charge fraction of bivalent cations (E_{BIV}) in gels: Thick stippled line represents slope in the paper by Prezzi et al. [17] for 30 days results for a microcrystalline quartzite. Symbols as in Figure 1.